

## Prediction of Mechanical Behaviour in Ni-Base Superalloys Using the Phase Field Model of Dislocations

V.A. Vorontsov<sup>1,a</sup>, R.E. Voskoboinikov<sup>2,b</sup> and C.M.F. Rae<sup>1,c</sup>

<sup>1</sup>Department of Materials Science and Metallurgy, University of Cambridge, Pembroke Street, Cambridge, United Kingdom, CB2 3QZ

<sup>2</sup>Institute of Materials Engineering, ANSTO, New Illawarra Road, Lucas Heights, NSW, Australia

<sup>a</sup>vassili.vorontsov@googlemail.com, <sup>b</sup>roman.voskoboinikov@gmail.com, <sup>c</sup>cr18@cam.ac.uk

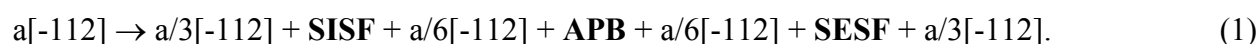
**Key words:** Primary Creep, Dislocations, Stacking Faults, Phase Field Modelling, Effective  $\gamma$ -surface

**Abstract.** The “Phase-Field Model of Dislocations” (PFMD) was used to simulate shearing of gamma-prime precipitate arrays in single crystal turbine blade superalloys. The focus of the work has been on the cutting of the  $L1_2$  ordered precipitates by  $a\langle 112 \rangle \{111\}$  dislocation ribbons during Primary Creep. The Phase Field Model presented incorporates specially developed Generalised Stacking Fault Energy ( $\gamma$ -surface) data obtained from atomistic simulations. The topography of this surface determines the shearing mechanisms observed in the model. The merit of the new  $\gamma$ -surface, is that it accounts for the formation of extrinsic stacking faults, making the model more relevant to creep deformation of superalloys at elevated temperatures.

### Introduction

Modelling of deformation behaviour, encompassing the full range of length scales, can reduce the empiricism involved in developing stronger superalloys. The Phase Field Model has proved a powerful tool for studying the deformation mechanisms in  $L1_2$  ordered superalloys on the scale of the dislocation interactions with precipitates [1,2]. The method has also been successfully applied to modelling  $\gamma'$  precipitate shearing by dislocations on the  $\{111\}$  plane [3] in single crystal superalloys and to study the role of channel plasticity during rafting [4,5] at higher temperatures and lower stresses ( $> 1000^\circ\text{C}$  and  $< 200\text{ MPa}$ ). However, the model, described in [3], had limited applicability to simulating  $\gamma'$  cutting at elevated temperatures, because it did not incorporate the formation of extrinsic stacking faults.

In particular, primary creep occurs via a mechanism known as ‘stacking fault shear’, whereby the  $\gamma'$  precipitates are cut by  $a\langle 112 \rangle$  dislocation ribbons that dissociate into partials that bind extensive superlattice intrinsic and extrinsic stacking faults (SISF and SESF respectively). Rae and Reed [6] propose the following example reaction, based on the work of Kear *et al.* [7,8] and TEM observations:



In second-generation superalloys, primary creep occurs at low temperatures ( $750\text{--}850^\circ\text{C}$ ) and high stresses  $\approx 750\text{ MPa}$ . A temperature-dependent threshold initiation stress of  $\approx 500\text{ MPa}$  is observed. The exact value correlates directly with the ability of the  $a\langle 112 \rangle$  dislocation ribbons to nucleate from  $a/2\langle 110 \rangle$  dislocations in the matrix. Once formed, they enter the  $\gamma'$  precipitates and shear them, leaving, no ‘debris’ when the shearing is complete.

This creep deformation regime is of substantial importance to industry, because it occurs to a significant extent in the “cold” webs of cooled “high-pressure” (HP) blades of aero-engines during take-off, climb and thrust reversal routines. Dislocations can propagate relatively uninhibited through both phases during this early stage of creep. In testing primary strains as high as 15% (depending on alloy and stress) [9] can be achieved due to the relatively large length of the  $a\langle 112 \rangle$  Burgers vector, the low fault energies associated with SISF and SESF, and the low dislocation density from the onset.

## Model Formulation

In PFMD dislocations are modelled as boundaries/interfaces between slipped and non-slipped regions, described in greater detail in [10]. Each slipped region is assumed to be a coherent misfitting ‘martensite platelet’ lying in the slip plane, which grows or shrinks in response to local and applied strain fields. The transformation strain field  $\varepsilon^0$  associated with the ‘platelet’ is a result of the Burgers’ vector  $b$  and is given by the following equation, where  $n$  is the slip plane normal and  $d$  is the slip plane spacing:

$$\varepsilon_{ij}^0 = (b_i n_j + b_j n_i) / d. \quad (2)$$

The phase field model determines the dislocation configuration by minimizing the total free energy  $F_{total}$  of the single crystal system containing dislocations subjected to an externally applied stress and has four contributing terms:

$$F_{total} = F_{elastic} + F_{gradient} + F_{crystal} - W. \quad (3)$$

$F_{elastic}$  is the elastic strain energy contribution. It describes the long-range interactions between the elastic strain fields associated with the dislocations. These can be mutual attraction or repulsion and result in their subsequent combination or annihilation. The elastic strain energy is solved using the Khachaturyan–Shatalov [11],[12] method.  $F_{gradient}$  is the gradient free energy and is responsible for the interface between slipped and non-slipped regions. A sharp interface would constitute a sharp Volterra dislocation core, but the gradient free energy provides a smooth interface around the platelet, on the slip plane, creating a smooth Peierls-Nabarro type core.

The crystal free energy  $F_{crystal}$  incorporates the periodic misfit potential that arises in the crystal in response to the atomic disregistry in the slipped region. This term describes the *local* state of the system: for instance whether there is a planar defect such as an APB or stacking fault. It thus governs the dissociation of perfect dislocations into partials and their subsequent interactions. Shen and Wang [13] have shown that data from atomistic simulations can be incorporated into  $F_{crystal}$  in the form of  $\gamma$ -surface functions:

$$F_{crystal} = \int (\gamma / d) \, dr. \quad (4)$$

The function  $\gamma$  used is a Fourier series fitted numerically to key symmetry points on the  $\gamma$ -surface obtained using atomistic simulation [14]. The valleys and local minima of the  $\gamma$ -surface give the minimum energy path for dislocation dissociation. Therefore its topography plays a key role in determining which shear mechanisms are active.

Lastly  $W$  is the elastic work done on the system by the applied stress.

The interplay between  $F_{crystal}$ ,  $F_{gradient}$  and  $F_{elastic}$  determines the core structure of the dislocations in the simulated crystal. The displacement components along the close-packed directions in the FCC crystal are given by field variables  $\eta$ . For the simulations dislocation activity on only the (111) slip plane was considered, which required only three field variables. The evolution of the system in time  $t$  is given by the time dependent Ginzburg-Landau equation, where  $M$  is a mobility coefficient:

$$\partial \eta / \partial t = -M (\delta F_{total} / \delta \eta). \quad (5)$$

### Extending the Model to Account for Extrinsic Fault Formation

In atomistic simulations, such as Density Functional Theory (DFT) or Molecular Dynamics (MD), a conventional  $\gamma$ -surface is obtained by displacement of two half-crystals relative to each other and measuring the associated energy density  $\gamma$  [15]. Vorontsov *et al.* used a phase field model with this type of  $\gamma$ -surface for  $\text{Ni}_3\text{Al}$  and Ni to investigate stacking fault shear in superalloys [3]. The study proved useful in identifying the effects of applied stress, dislocation character and precipitate geometry on the shearing mechanism. However, the work also highlighted the necessity for a new  $\gamma$ -surface that could allow PFMD to reproduce the extended SESF faults. The SESF is a low-energy two-layer fault with stacking sequence ABCBABC. However on the conventional  $\gamma$ -surface its position is taken by the single-layer high-energy fault with the energetically undesirable stacking sequence ABCCABC and a high local maximum, rather than minimum, on the  $\gamma$ -surface.

Creation of extrinsic stacking faults requires displacement of atoms on the plane adjacent to the slip plane. Therefore the conventional approach of calculating a  $\gamma$ -surface is inadequate, because the new surface has to incorporate movement of atoms on two planes. To solve this problem Voskoboinikov and Rae [16] have developed an effective two-layer  $\gamma$ -surface for the  $\{111\}$  plane in both pure Ni and  $\text{Ni}_3\text{Al}$ . MD simulation was implemented using the Mishin EAM potential for the Ni-Al system [17]. The key difference from conventional methods was the introduction of a single floating plane between the two half crystals. For every relative displacement of the half crystals the middle plane position was adjusted to give the lowest possible energy density. The end result was an effective  $\gamma$ -surface that featured both intrinsic and extrinsic stacking faults.

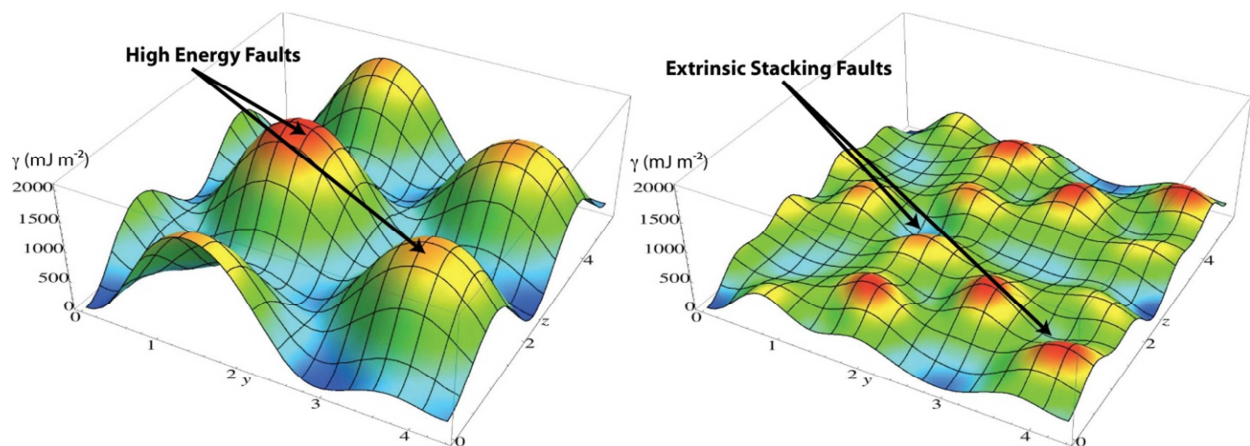


**Fig 1:** Comparison of 1-layer (left) and 2-layer effective (right)  $\gamma$ -surface functions for  $\text{Ni}_3\text{Al}$ . The latter gives a lower overall energy density and more possibilities for dissociation into partial dislocations.

Again a Fourier series was fitted to the MD data to give the  $\gamma$  function in  $F_{crystal}$ . The extrinsic faults added new local minima, thus creating new pathways for dislocation dissociation.

Phase field simulations were carried out to test the new two-layer  $\gamma$ -surface functions. Pure Ni was used for the  $\gamma$  matrix and  $\text{Ni}_3\text{Al}$  was chosen for the  $\gamma'$  precipitates. Two distinct sets of simulations were carried out. In the first, both the matrix and precipitate phases had a two-layer  $\gamma$ -surface. In the other set, the matrix phase used a single-layer  $\gamma$ -surface, while the  $\gamma'$  had the two-layer  $\gamma$ -surface. The purpose of this was to investigate cases where movement of atoms on the adjacent plane is activated at different conditions (e.g. temperature). Pairs of  $a/2\langle 112 \rangle$  dislocations were introduced in the matrix and allowed to propagate through the phases under varying values of applied stress. Dislocation ribbons of both edge and mixed ( $60^\circ$  screw) character were studied.

Figure 2 shows four stages, left to right, during the passage of the dislocation ribbon through the precipitate either in the edge (triangle resting on base) or the mixed  $60^\circ$  screw configuration (triangle on corner). The first three examples compare mixed configurations for (i) the single layer model, (ii) the single layer  $\gamma$ /double layer  $\gamma'$ , and (iii) the double layer throughout. The last two show edge dislocations with (iv) single layer  $\gamma$ /double layer  $\gamma'$  and (v) double layer throughout.

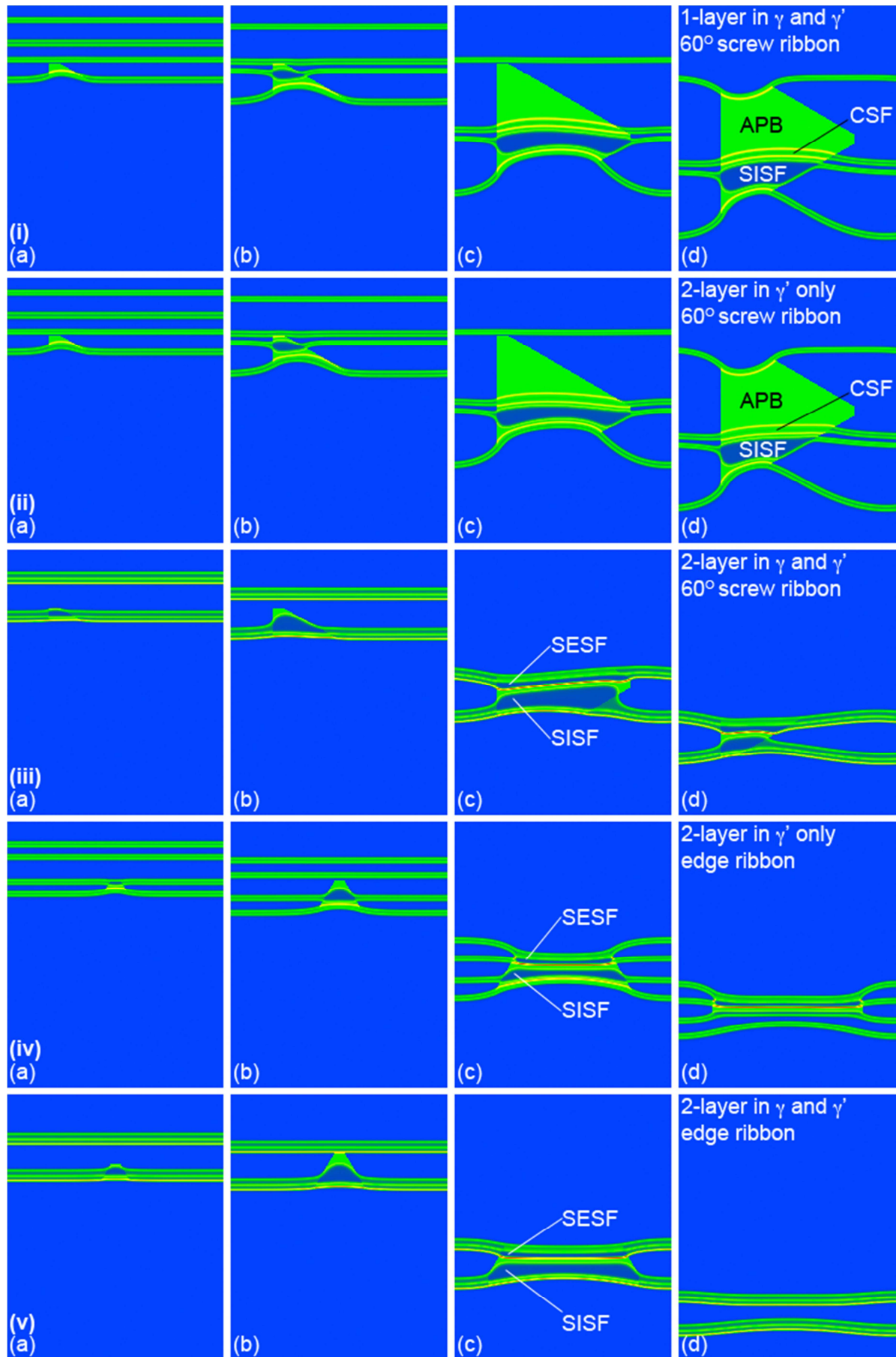


**Fig 2:** Comparison of shearing mechanisms obtained using different types of  $\gamma$ -surface for  $60^\circ$  screw and pure edge  $a\langle 112 \rangle$  dislocation ribbons.

The modelling has shown that the creation of extrinsic stacking faults is energetically favourable during the shearing of the simulated alloy by the mixed dislocation ribbons, but only when the two-layer  $\gamma$ -surface is used for the matrix phase. In this case, Fig. 2(iii), the  $a/2\langle 112 \rangle$  dislocations are stable in the matrix phase and do not dissociate into pairs of  $a/2\langle 110 \rangle$  dislocations. In comparison, using a single-layer  $\gamma$ -surface in the  $\gamma$  phase, the  $a/2\langle 112 \rangle$  dislocations dissociate into different  $a/2\langle 110 \rangle$  dislocations, (compare Fig. 2(i) and (ii) with Fig. 2(iii)) and separate quite widely. This is not surprising as the force on the two component  $a/2\langle 110 \rangle$  dislocations is different in the mixed case. Upon cutting of the  $\gamma'$  precipitate the formation of extrinsic SESF fault was found to be favourable, but only in the case where they already existed in the matrix as part of the  $a/2\langle 112 \rangle$  dislocation.

In the case of the edge dislocations, the situation is rather different. The SESF is formed in the  $\gamma'$  in both cases, whether or not the single layer  $\gamma$  surface was used in the  $\gamma$  matrix phase, Fig. 2(iv) and 2(v). Here the force on the two component  $a/2\langle 110 \rangle$  dislocations in the matrix phase is equal and they do not tend to separate as much as they do in mixed dislocations. But it is clear that the introduction of the double layer  $\gamma$  surface has stabilised the  $a/2\langle 112 \rangle$  dislocation. There is distinct (blue) perfect lattice between the  $a/2\langle 110 \rangle$  dislocations in Fig. 2(iv) but not in Fig. 2(v). Nevertheless, the SESF forms as the dislocations enter the  $\gamma'$  phase. The difference from the mixed case above, Fig. 2(ii), is that the dislocations, although distinct, remain close and are hence able to combine and form the SESF. Hence, it would appear to be that it is the proximity of the necessary dislocations which is important, not the prior existence of an extrinsic fault in the matrix.

When slip in the matrix is limited to intrinsic faults only, the formation of the SESF was sensitive to the character of the dislocation ribbon. It was favoured in the case of edge dislocation but not in that of mixed character.

The widths of the two stacking faults in the  $\gamma'$  phase, the SESF and SISF, are slightly different, with the SISF being the wider. This reflects the lower energy of this fault on the  $\gamma$  surface. What is noticeable, is that the trailing SESF is not widely extended, as is seen in the ribbons observed in deformed microstructures. Often, the trailing  $a/6\langle 112 \rangle$  dislocation lies at the  $\gamma/\gamma'$  interface and can be a full precipitate width behind the preceding dislocation. It is not possible to lower the SESF energy sufficiently to give this separation as the line tension of the trailing dislocation alone would cause it to cut through the precipitate.

An important point is that the model does not address the activation barrier for slip producing extrinsic stacking faults. It merely gives the lowest energy configuration, and does not describe physically how this configuration is achieved mechanistically. The creation of the low energy SESF in the  $\gamma'$  phase by pure shear is difficult to achieve, because it can require a large displacement of atoms on the adjacent plane by a Burger's vector of  $a/2\langle 112 \rangle$ . Alternatively, Kovarik *et al.* [1] propose that vacancy-mediated diffusion mechanism of atomic reordering that creates the SESF without such a large displacement. Such a mechanism would require time to occur delaying the formation of the SESF, but equally would require the reverse process, as the SESF was removed by the trailing  $a/6\langle 112 \rangle$  dislocation. This would explain why the SESF extends much more widely in practice than is feasible on the basis of fault energies alone. Thus an improved model will incorporate dynamic temperature dependent switching between the two types of  $\gamma$ -surface, to account for the underlying reordering transitions that must take place.

The  $\gamma$ -surface functions used in the model are fitted to arbitrarily selected fault energies. For the purpose of the simulations the fault energies were taken from MD simulations. However, commercial alloys contain as many as ten elements, each of which has an effect on the various fault energies. Thus the  $\gamma$ -surface functions will need to be adjusted to alter the energy of the individual planar faults, maintaining the remaining topology. By observing equilibrium dislocation configurations in TEM specimens of superalloys, PFMD can prove a very useful tool in identifying and isolating the effects of the various alloying additions on creep strength.

## Conclusion

The existing PFMD has been successfully extended to modelling formation of extrinsic stacking faults by incorporating the newly developed effective two-layer  $\gamma$ -surfaces for Ni and Ni<sub>3</sub>Al. This has enabled the model to study more accurately the shearing mechanisms that are active in superalloys at elevated temperatures. The modified model offers plenty of opportunity for further research, especially if used in conjunction with experimental observations.

## Acknowledgements

The authors would like to acknowledge funding from the EPSRC (UK) under grant number EP/D04619X/1. Also, V. Vorontsov would also like to thank Prof. Y. Wang and Dr. N. Zhou of the Ohio State University and Prof. G. Schoeck from the University of Vienna for their advice and assistance with the aforementioned research.

## References

- [1] L. Kovarik, R.R. Unocic, Ju Li, P. Sarosi, C. Shen, Y. Wang and M.J. Mills, *Progress in Materials Science*, Vol. 54, p. 839-873, (2009)
- [2] R.R. Unocic, L. Kovarik, C. Shen, P.M. Sarosi, Y. Wang, J. Li, S. Ghosh and M.J. Mills, *Superalloys 2008*, p. 377-385, (2008)
- [3] V.A. Vorontsov, C. Shen, Y. Wang, D. Dye and C.M.F. Rae, *Acta Materialia*, Vol. 58, p. 4110-4119, (2010)
- [4] N. Zhou, C. Shen, M.J. Mills and Y. Wang, *Acta Materialia*, Vol. 55, p. 5369-5381, (2007)
- [5] N. Zhou, C. Shen, M.J. Mills and Y. Wang, *Acta Materialia*, Vol. 56, p. 6156-6173, (2008)
- [6] C.M.F. Rae and R.C. Reed, *Acta Materialia*, Vol. 55, p. 1067-1081, (2007)
- [7] B.H. Kear, A.F. Giamei, G.R. Leverant and J.M. Oblak, *Scripta Metallurgica*, Vol.3, p. 123-129, (1969)
- [8] B.H. Kear, A.F. Giamei, G.R. Leverant and J.M. Oblak, *Scripta Metallurgica*, Vol. 3, p. 455-460, (1969)
- [9] C.M.F. Rae, K. Kakehi and R.C. Reed, "On the effect of rhenium on the extent of primary creep in advanced Ni-based superalloys.", *Materials for advanced power engineering (Proceedings)*, p. 207-16, (2002)
- [10] Y.U. Wang, Y.M. Jin, A.M. Cuitiño and A.G. Khachaturyan, *Acta Materialia*, Vol. 49, p.1847-57, (2001)
- [11] A.G. Khachaturyan, "Theory of transformations in solids.", Dover Publications Inc., (1983)
- [12] J.D. Eshelby, *Proc. Roy. Soc. A*, Vol. 241, p. 376-96, (1957)
- [13] C. Shen and Y. Wang, *Acta Materialia*, Vol. 52, p. 683-91, (2004)
- [14] G. Schoeck, S. Kohlhammer and M. Fähnle, *Philosophical Magazine L.*, Vol. 79, p. 849-57, (1999)
- [15] V. Vitek, *Philosophical Magazine*, Vol. 18, p. 773-86, (1968)
- [16] R.E. Voskoboinikov and C.M.F. Rae, *IOP Conf. Ser.: Mater. Sci. Eng.*, Vol. 3, (2009)
- [17] Y. Mishin, *Acta Materialia*, Vol. 52, p. 1451-67, (2004)